ISSN 1573-160X, *PHYSICAL OCEANOGRAPHY*, Vol. 30, Iss. 5, pp. 594-611 (2023)
Original Russian Text © L. A. Petrenko, I. E. Kozlov, 2023,
published in *Morskoy Gidrofizicheskiy Zhurnal*, 2023, Vol. 39, Iss. 5, pp. 631–649.

Original article

Variability of the Marginal Ice Zone and Eddy Generation in Fram Strait and near Svalbard in Summer Based on Satellite Radar Observations

L. A. Petrenko ✉, I. E. Kozlov

Marine Hydrophysical Institute of RAS, Sevastopol, Russian Federation
✉ *larcpetr@gmail.com*

Abstract

Purpose. The aim of the study is to investigate the spatial and temporal variability of drifting ice field edge and the features of eddy generation in the marginal ice zone (MIZ) in Fram Strait and near Svalbard during the warm period in 2007.

Methods and Results. Satellite radar images of Envisat ASAR for June – September 2007 were used to fix the position of drifting ice field boundary and to reveal the surface manifestations of eddy generations in the MIZ. It is established that during the upper mentioned period, the ice – water boundary experienced unequal displacements along its entire length, and that a total range of the ice edge movements was 30–220 km. At different wind conditions, the ice edge motion was accompanied by the formation of ice filaments and eddies, the maximum number of which was recorded in June. The data analysis allowed us to identify more than 2000 pronounced MIZ eddies in which the structures with a cyclonic type of rotation were evidently predominant (78%). The larger eddies (10–20 km in diameter) were observed over the deep-water areas of Fram Strait and over the Greenland Sea shelf, whereas the smaller ones (~ 5 km in diameter) – in the coastal areas of Svalbard. The cases when the ice fragments were detached from the ice field and subsequently involved in the vortex motion were recorded. The ice drift and orbital motion velocities in the eddies were assessed.

Conclusions. The ice edge displacements and the process of eddy generation in the MIZ are significantly affected by the wind conditions. When the wind direction changes abruptly, the ice field fragments can be detached. The identified MIZ eddies are mainly of cyclonic rotation direction.

Keywords: marginal ice zone, ice edge, eddies, Svalbard, Fram Strait, satellite radar images, Arctic Ocean

Acknowledgements: The present study was carried out with support of the RSF grant No. 21-17-00278 (analysis of spatial and temporal variability of the marginal ice zone, eddy fields and their relationship with the background wind conditions). Data collection and processing, and eddy identifications using satellite data were performed within the framework of state assignment No. FNNN-2021-0010.

For citation: Petrenko, L.A. and Kozlov, I.E., 2023. Variability of the Marginal Ice Zone and Eddy Generation in Fram Strait and near Svalbard in Summer Based on Satellite Radar Observations. *Physical Oceanography*, 30(5), pp. 594-611.

Introduction

The marginal ice zone (MIZ) is a transition region from open ocean to dense ice cover with typical sea ice concentration values of 20–80%. This is an area of active interaction between the atmosphere, ocean, and ice, which determines the spatial position of the ice distribution boundary.

The ice cover area in Fram Strait and near Svalbard varies significantly throughout the year, decreasing in summer and increasing significantly in winter. The region, within which the shifts of the ice distribution boundary occur, is

distinguished by significant wind variability and sharp gradients of thermohaline characteristics in the surface layer of the ocean [1–4].

At the winds “from ice to water” and winds directed along the edge when the ice is located on the left, there is a significant decrease in the sea ice concentration inside the ice zone, and the ice shifts towards open water [5], where the melting process accelerates due to the fact that ice-free water has higher salinity and higher temperature, including due to radiation heating [6]. The resulting gradients contribute to the formation of eddies of various types of rotation.

During the winds directed from the ice-free water to the ice, and winds along the edge with the ice located on the right, as a result of convergence, the edge of the ice field becomes compacted. At the same time, individual ice floes, shifting towards the main ice cover, collide and break up into smaller ones, which also stimulates the melting and desalination of the sub-ice layer, and the aggravation of density gradients [7], contributing to the activation of meso- and submesoscale processes in the ocean. These processes can be studied using ocean remote sensing methods from space, the most effective of which is the analysis of satellite synthetic-aperture radar (SAR) data [8–10]. Identification of dynamic processes inside the MIZ based on SAR data is possible both on the basis of expert assessment by visual detection of their radar signatures [11, 12] and in an automated way based on machine learning methods [13, 14].

An important advantage of satellite SAR data is their high spatial resolution and independence from cloudiness and illumination conditions, which allows for a joint analysis of the spatial and temporal variability of the MIZ and eddy generation processes in the area under study.

Data and methods of their processing

In this work, the radar images obtained from the Envisat ASAR satellite in *C*-band and Wide Swath Mode (WSM) (swath width 400 × 400 km, spatial resolution 150 × 150 m) in June – September 2007, were used. High-resolution wind speed field data were obtained from the original radar images based on the CMOD4 model function using wind direction from the NCEP reanalysis data.

A total of 448 SAR images of the water area in Fram Strait and near Svalbard were processed in the area with coordinates 75–82°N, 13°W – 30°E. Coverage of the study area by satellite SAR survey (the number of images in the nodes of the grid of 300 × 300 points within the coordinates of the area under consideration) is shown in Fig. 1. It can be seen that the central and northeastern parts of the study area, which account for over 100 SAR images, were covered with data more informatively. The western, eastern, and southern parts have less satellite information, 40–80 radar images. The minimum data availability is observed near the ice edge, where the coverage density, due to the seasonal dynamics of the ice cover, is 10–40 images for the entire period.

Using satellite data, the spatial position of the ice distribution boundary (edge of the ice field) was visually recorded. The position of the ice distribution boundary was taken as the ice edge, reflecting the ice – open water transition.

Surface manifestations of eddy structures (SMES) in the MIZ were also identified, the coordinates of the center of the eddies, their diameter, direction of rotation, and the depth of the place corresponding to the eddy center were

determined. The characteristics of eddy structures were specified based on the technique described in [9].

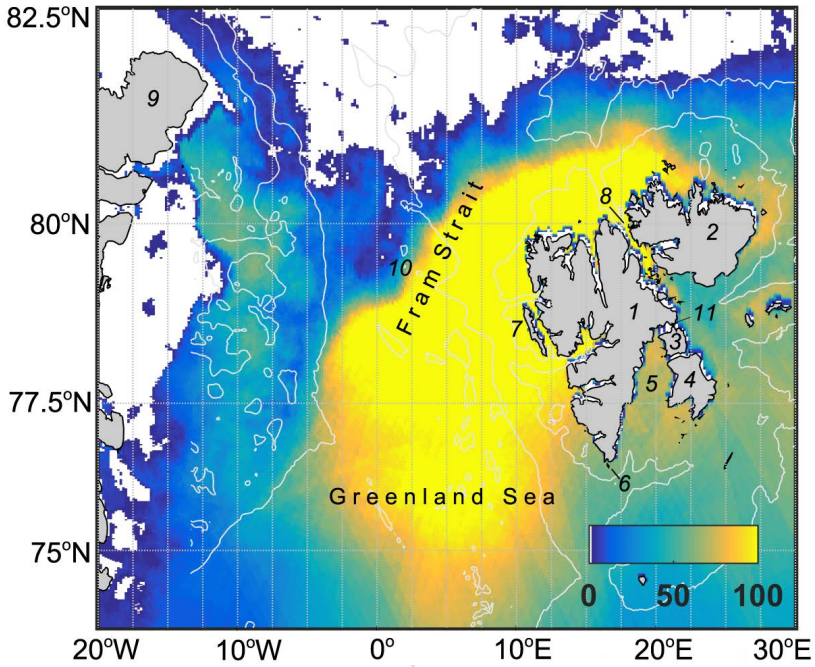

F i g. 1. Satellite SAR imagery of the area under study (number of images in the grid nodes of 300 × 300 point). Designations: *1* – Spitsbergen Island; *2* – North-East Land Island; *3* – Barents Island; *4* – Edge Island; *5* – the Stur-Fjord Strait; *6* – Serkappeya Island; *7* – Prince Charles Foreland; *8* – the Hinlopen Strait; *9* – Greenland Island; *10* – the Molloy Deep; *11* – the Heleysunn Strait

Variability of the ice distribution boundary

Due to the fact that the SMES from satellite radar images are distinguishable in open water areas and in areas of low ice concentration [2, 9, 11], to study the spatial distribution of eddies, the position of the ice field edge was recorded in order to obtain a general picture of the distribution of drifting ice within the area under consideration.

The 2007 warm period was distinguished by the minimum ice cover in the Arctic Ocean for all previous years, i.e., the maximum open water area. In the period from June to September 2007, the polar anticyclone was shifted southward of the Canada Basin center (Fig. 2) [15]. At the same time, cyclones moving across the continental part caused advection of air masses from warm continents to the Arctic [16–18]. As a result, a zone of increased pressure gradients arose (Fig. 2, *a*), which is typical in the years with minimal ice cover and contributes to intensive removal of ice through Fram Strait (Fig. 2, *b*) [15, 19], since the movement of ice under the weather situation that developed in 2007, occurred along atmospheric isobars [1] [20].

[1] Colony, R.L. and Rigor, I.G., 1993. *International Arctic Buoy Program Data Report for 1 January 1992 – 31 December 1992*. Technical Memorandum APL-UW TM29-93. Seattle, Washington: Applied Physics Laboratory, University of Washington, 215 p.

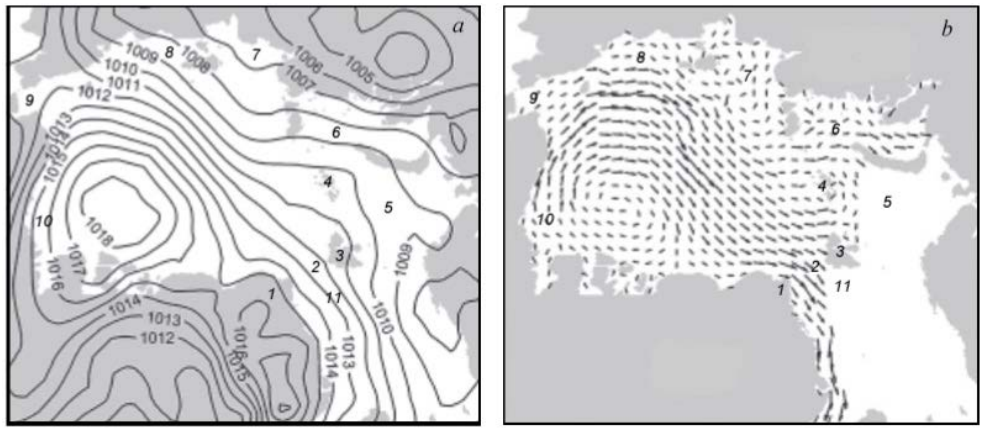

F i g. 2. Fields of the atmospheric pressure (*a*) and the ice drift velocities (*b*) over the Arctic Ocean averaged for May – September 2007, derived from [15]. Designations: *1* – Greenland Island; *2* – Fram Strait; *3* – Svalbard; *4* – Franz-Josef Land; *5* – the Barents Sea; *6* – the Kara Sea; *7* – the Laptev Sea; *8* – the East Siberian Sea; *9* – the Chukchi Sea; *10* – the Beaufort Sea; *11* – the Greenland Sea

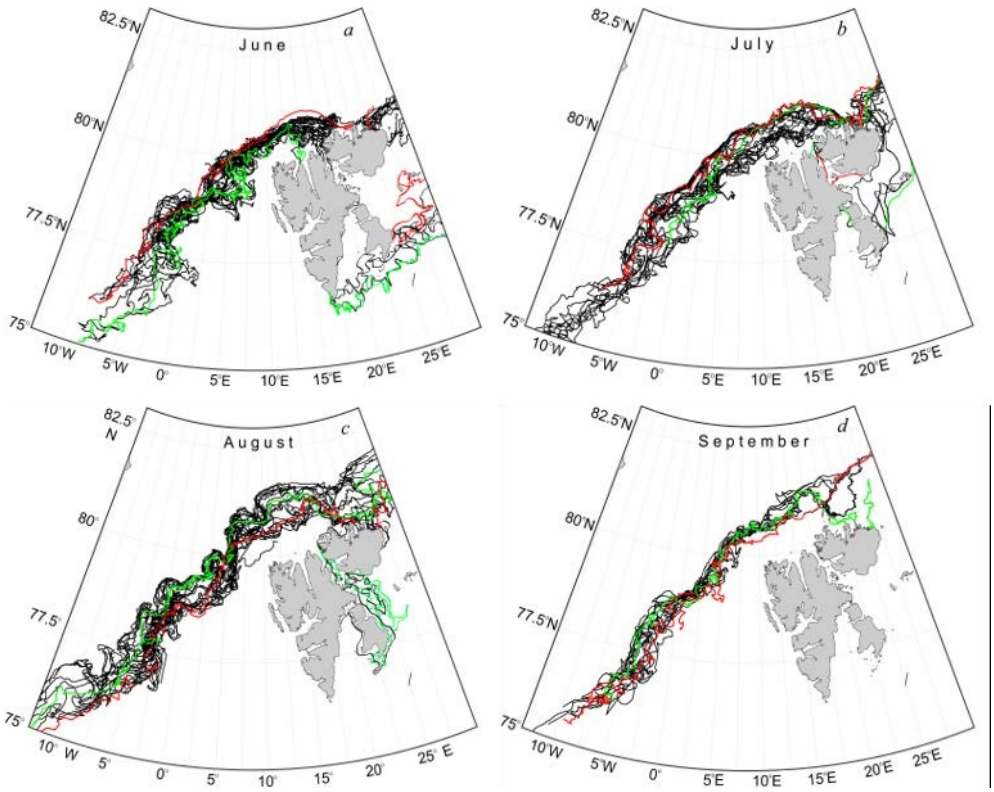

F i g. 3. Spatial variability of the ice edge in Fram Strait region and near Svalbard in June (*a*), July (*b*), August (*c*) and September (*d*) 2007. The ice edge position at the beginning of a month is indicated in green and at the end of a month – in red

Analysis of satellite data obtained in Fram Strait and near Svalbard in June – September 2007 revealed that the edge of the drifting ice field is subject to strong deformations, and its displacement occurs unequally along its entire length (Fig. 3).

At the beginning of June 2007, the ice field edge northward of Svalbard was located at 80.5°N and adjoined the shore at Cape Verlegenhuken (16.25°E). The water area on the eastern side of the archipelago was completely occupied by ice up to 77°N. In the south, the ice extended to the very southern tip of Svalbard – Sörkappoya Island (76.5°N, 16.57°E). During June 2007, intense ice loss took place in the south and southeast of the archipelago. By the end of the month, the Storfjord Strait was free of ice, and the ice boundary moved northward to 78°N on the eastern side (Fig. 3, *a*).

Westwards from the archipelago, the orientation of the drifting ice field edge in the direction from northeast to southwest is determined mainly by the interaction of the main currents: relatively cold polar waters of the East Greenland Current (EGC) and the West Spitsbergen Current (WSC) carrying the relatively warm Atlantic waters (AW) [21].

In June 2007, at prevailing weak winds, the nature of deformations and spatial displacement of the ice field edge reflected the general picture of the AW transport in the area under study. In Fig. 3, *a*, it is clear that the ice edge in Fram Strait is shifted towards the west under effect of warm recirculation branches of the WSC. Among them, there are well-developed ice filaments in the area of 77–79°N, directed towards the ice-free water area and caused by the EGC effect on the outflow from the polar region. Since the EGC propagates along the isobaths of the East Greenland shelf slope, the formation of filaments occurs at points of sharp change in the curvature of the isobaths when the external jet is separated from the general EGC flux under effect of local winds [19, 22].

The edge configuration in June reflects clearly the presence of a large eddy generation in the region of the Molloy Deep (MD) (79°N, 2.5°E) (Fig. 3, *a*).

Northwards from Svalbard, the edge of the ice field retreated not only to the north, but also to the east. During June 2007, the eastern boundary of the ice shifted from Cape Verlegenhuken (16°E) towards Cape Platen (23°E), i.e., by 135 km. At the same time, the ice retreat to the north in this area amounted to ~ 200 km (up to 81°E). The greatest ice edge retreat to the north was observed parallel to the Hinlopen Strait axis and was caused by increased wind when passing through a narrow and long strait.

At the end of June, northwards of Svalbard (80.68° N), in the area of shallow depths located at 20–27°E, a residual ice field, bordering the area of ice-free water from the west and east, i.e., an ice “bridge” (Fig. 4, *a*), was formed. Depending on the wind direction, this “bridge” was predominantly of fast ice nature or was separated from Svalbard by a narrow polynya.

By the end of June, the edge of the drifting ice field in Fram Strait was compacted and leveled along its entire length under the effect of prolonged moderate easterly winds.

In the first ten days of July, the wind of changing direction caused movements of the ice field edge, which contributed to the emergence of numerous eddy structures in the marginal ice zone [23]. As a result, in July the ice edge northwards

from 79.5°N practically retained its northernmost position with a displacement range of ~ 80 km.

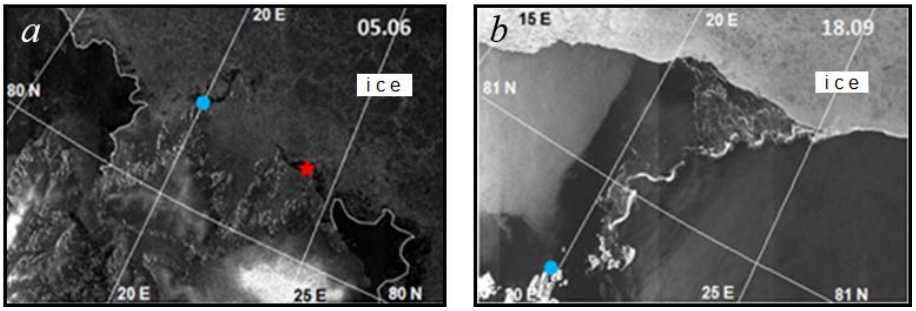

F i g. 4. Satellite image of the ice boundary position north of Svalbard on June 5 (*a*) and September 18 (*b*), 2007. Cape Nordkapp is marked in blue, Cape Platen – in red, and the ice boundary – by a white line

Southwards from 79.5°N, the retreat of the drifting ice field boundary into Fram Strait continued, and the range of fluctuations in its position reached 200 km. The minimum width of the displacement zone in July (66 km) occurred at points with coordinates of 76.4°N, 4.5°W (45 km), and 79.8°N, 3.75°E (Fig. 3, *b*).

In the Hinlopen Strait, ice persisted until the end of July. Only a change in the prevailing winds southeastwards of Svalbard in August, which intensified the influx of warm waters from the south, led to an acceleration of the melting process and the clearing of the strait from ice.

The seasonal retreat of the ice boundary leading to an increase in the ice-free water area, occurred until the first days of August, after which the direction of the shift changed to the opposite one. In August, the range of edge displacements was 130–140 km along almost the entire length of the ice field boundary, with a minimum of 30 km at 79.9°N, 6.25°E.

In September, the greatest ice field boundary shifts were observed southwards from 79°N. The width of the displacement zone reached 90 km. Northwards from 79°N, the fluctuations in the ice edge occurred within 55 km. Northwards from Svalbard, the edge retreat continued in September and amounted to more than 120 km.

In the second ten days of September 2007, the ice “bridge” beyond 20°E by September 18, 2007 degenerates into a thin strip of melting ice (Fig. 4, *b*), stretching towards the shore from the compacted edge of the ice field and showing the position of the collision site of multidirectional surface flows, and then completely disappears.

Fig. 5 demonstrates the ice edge displacement north of Svalbard by showing variability of the ice field boundary distance from three different points of the archipelago – the northernmost point of Amsterdam Island (79.78°N, 10.75°E), Cape Verlegenhuken (80.06°N, 16.25°E), and Cape Platen (80.51°N, 22.79°E). It can be seen that off the northern coast of Svalbard, the ice retreat to the pole was interrupted twice during the 2007 summer period – in the first ten days of July and in the second ten days of August. At the same time, the ice mass again occupied the northeastern shelf of the archipelago.

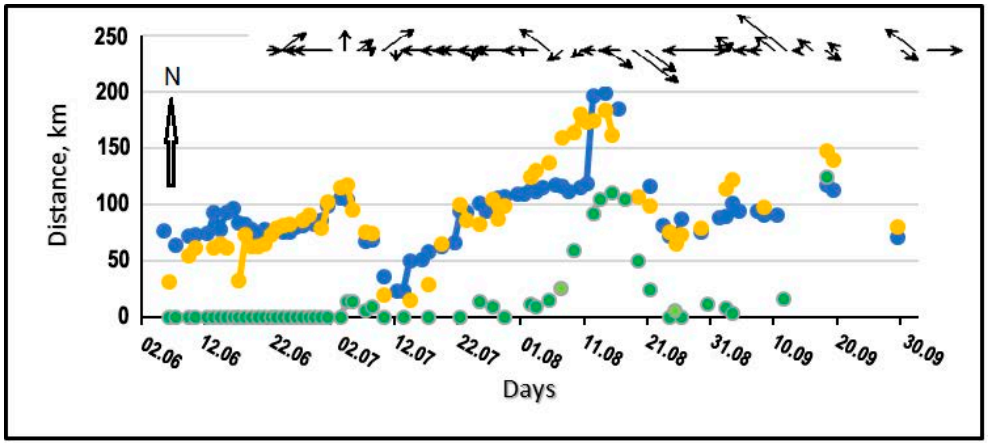

F i g. 5. Distance of the ice edge from the Svalbard Archipelago northern coast: from the Amsterdam Island (blue), from Cape Verlegenhuken (yellow), and from Cape Platen (green). Mean daily wind vector is indicated by the arrows

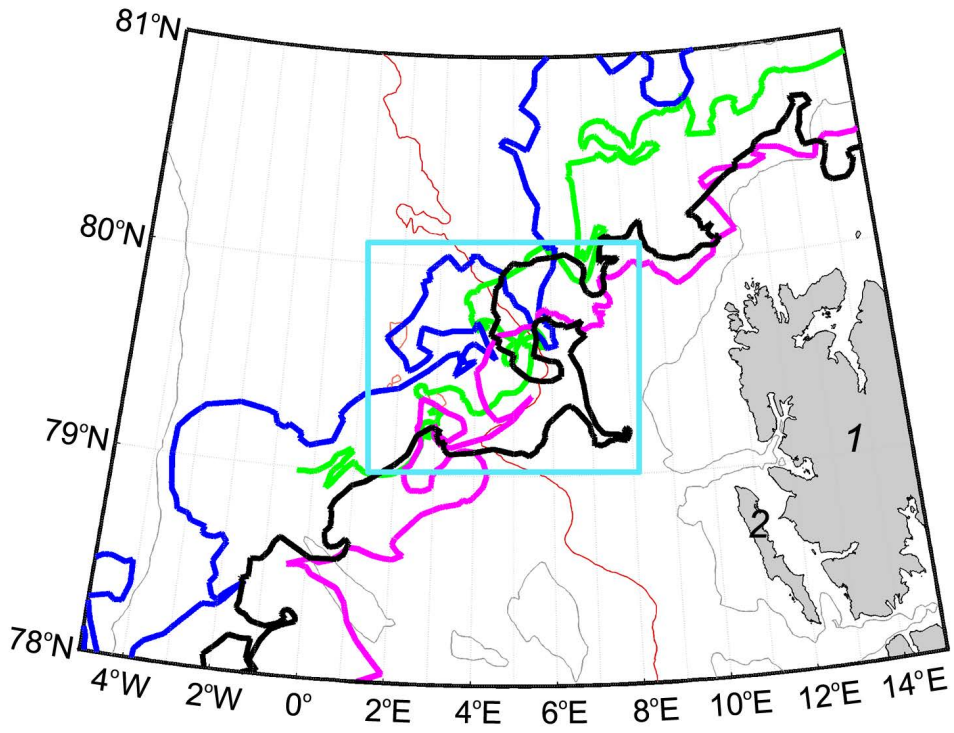

F i g. 6. Manifestation of the quasi-stationary eddy at the ice edge in the vicinity of the Molloy Deep (highlighted in cyan) during the warm period in 2007: on June 3 (black); on July 9 (magenta); on August 9 (blue), and on September 6 (green). Designations: the 2000 m isobath is marked in red; *1* – Spitsbergen lsland; *2* – Prince Charles Foreland

Throughout the summer period, the deformation of the drifting ice field edge was affected by eddy structures – both formed in the marginal ice zone and advected to the ice edge. As a result, ice was involved into the eddy movement when its concentration was low, and at a sufficiently dense edge, eddies with warm water caused active melting of the ice and were "imprinted" on the edge of the ice field.

According to satellite images, it was noted that in Fram Strait, in the MD area, the configuration of the ice edge periodically reflected the presence of a quasi-stationary cyclonic eddy on the water surface, which was defined as topographically trapped eddy (Fig. 6). It is also a part of a large-scale eddy movement consisting of recirculating AW and generated by the bottom topography features at the MD periphery [24]. This work also presents the ice edge configurations in the eddy area, obtained in different years, and concludes that the surface manifestation of eddy depends on the acting wind and the variability of background currents. In this case, shifts in the eddy position occur mainly towards the west and northwest.

A number of eddy manifestations in the vicinity of the MD during the period under consideration was observed for three days in June (June 3, 8, and 9), one day in July (July 9), 12 days in August (August 2–13), one day in September (September 6). In August, the high frequency of eddy occurrence was due to the predominance of southeasterly and easterly winds in the first half of the month, which led to the eddy intensification due to the intensification of the drift component of surface currents, in particular of the AW recirculation branch that went around the eddy [21, 25].

Eddy manifestations within the MIZ occurred in various ways. In Fig. 6, the contours of the ice edge on individual days of the 2007 warm period in the MD area are demonstrated. On the indicated days, the region was characterized by weak winds (2–3 m/s). It can be seen that the eddy appeared more clearly in June and August when a cyclonic wind vorticity caused by northerly winds in Fram Strait and southerly winds off the Svalbard coast was present. In July and September, the presence of the eddy was only indicated by a notch on the ice edge. The surface manifestation of the eddy was weakly expressed on September 6 under anticyclonic wind vorticity (a southerly wind in the strait and the northerly one near Svalbard), and on September 9 under weak northerly winds over the entire region. Thus, it can be assumed that the manifestation of an eddy on the sea surface in the MD region depends not only on the wind direction and speed, but also on the sign of its vorticity.

In some cases, the absence of eddy manifestations at the ice edge could be related to the intense drift currents suppressing the eddy-induced circulation pattern at the sea surface [21].

During the study period, we also recorded some cases when the eddies were able to detach the sea ice from the main ice field and carry it away into the open water. Fig. 7 illustrates how a fragment of the ice field was involved into the eddy movement by an anticyclonic eddy (formed on ice-free water) with a diameter of > 40 km. The initial area of the fragment was about 960 km^2.

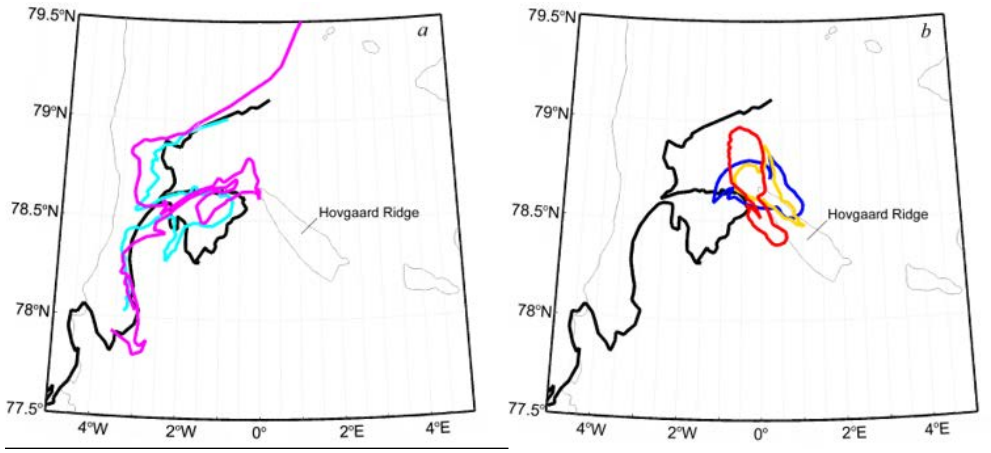

F i g. 7. Involvement of ice from MIZ in the eddy motion (*a*) and its trapping by the anticyclonic eddy (*b*). The ice edge position on July 26 is shown in black; the contour of the involved ice on July 27 – in cyan, on July 28 – in magenta, on July 29 – in blue, on July 30 – in yellow, and on July 31 – in red

The process of ice involvement into the eddy began on July 26, 2007 (Fig. 7, *a*) at a compacted edge under effect of the northeasterly wind. After wind direction changed to southwestern on July 29, a fragment was detached from the ice mass, followed by involvement in the rotation of an anticyclonic eddy that formed over a submarine elevation. The ice area in the eddy at that moment was already 801 km^2. Until almost complete disappearance of ice, the eddy remained stationary in the area of the northern end of Hovgaard Ridge. The stretching of the melting ice remnants with the wind on July 31 (Fig. 7, *b*) indicated that the eddy movement had ceased. The rotation speed in the eddy, estimated from successive images for July 30, reached 23 cm/s. The lifetime of the anticyclonic eddy was about 6 days.

Another case of ice detachment from the MIZ was observed in early August 2007 north of Svalbard. In this area, the position of the ice boundary can change sharply under effect of southerly and southeasterly winds, intensified when passing through the long and narrow Hinlopen Strait. Thus, at the end of July, the edge of the drifting ice field was exposed to the southeasterly wind strengthened by the strait, which led to its meandering (Fig. 8, *a*).

A southward oriented filament stretching from the MIZ and gradually evolving into cyclonic eddy was formed as a result of wind pumping in the region of 8–9°E. North of Svalbard on August 1, the wind direction changed to northeasterly leading to the eddy separation. After detachment, the ice fragment with an initial area of ~ 95 km^2 moved along the edge toward northwest under the combined action of the northern WSC branch and the eastern wind. The drift velocity of the ice fragment averaged 14 cm/s. At the same time, the ice edge acquired a pronounced wavy configuration (Fig. 8, *b*). The occurrence of this type of deformation was studied using numerical modeling in [26]. It was found that the wave-like deformations at the ice edge were caused by the wind-wave effect on the meandering edge of the broken ice field. When exposed to wind and waves at

an acute angle to the ice edge, the ice is squeezed out differently. The displacement is minimal (maximal) when the ice edge is located along (perpendicular to) the wind/wave direction (Fig. 8, *c*). In this particular case, the ice shifted westward at about 5–13 km/day velocity. The distance between the "crests" of such waves at the edge was about 130–140 km. Such wave-like ice edge deformations reached 50–60 km deep into the ice field.

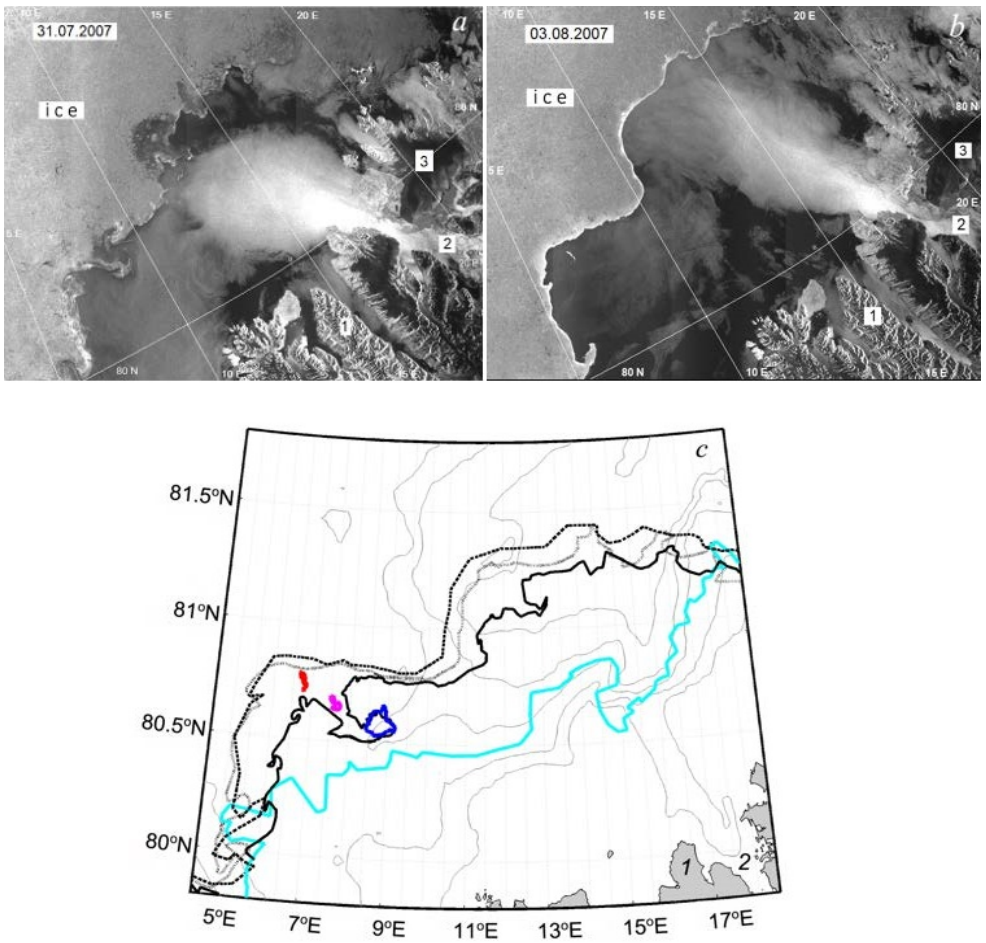

F i g. 8. Variability of ice boundary to the north of Svalbard based on satellite data for July 31 (*a*) and August 03 (*b*); on fragment (*c*), the ice edge on August 1 is shown by a solid line, on August 2 – by a dotted line, on August 3 – by a dashed line, and in late August – by cyan color; position of the ice field fragment on August 1 is shown by blue, on August 2 – by magenta, on August 3 – by red. Designations: *1* – Spitsbergen Island, *2* – the Hinlopen Strait, *3* – North-East Land Island

Eddy generation east of Svalbard was mainly driven by density gradients developed at the ice edge. Another obvious cause for the generation of eddy structures is the interaction of tidal currents and the East Spitsbergen Current (ESC) with bottom topography features and islands [27, 28].

Eddy generation in the marginal ice zone

The eddy generation in the MIZ could be caused by many possible mechanisms – barotropic and baroclinic instability of surface currents along the MIZ, topographic generation, interaction of advected AW eddies with melt water fronts, Ekman wind pumping at the ice edge or a combination of the above causes [21, 25, 29, 30].

To analyze the statistics of eddy generation in the MIZ, 294 images were selected from 448 Envisat ASAR satellite images of the study area. As a result of their processing, 2272 surface manifestations of eddies in the MIZ of Fram Strait and near Svalbard were identified. By month, 1162 eddies were identified in June, 420 – in July, 451 – in August, and 239 – in September.

1071 (832) eddy structures were identified in places with depths below 300 (200) m. In deep water with depths above 1000 m, 852 eddies were identified. As can be seen in the histogram of the dependence of the number of identified eddies on the total water depth at their detection location (Fig. 9, *a*), the maximum number of eddy structures was observed above the depths of up to 400 m, which indicates the impact of the bottom relief features on their generation. The second maximum occurs at depths of 2500–3000 m, corresponding to the central part of Fram Strait. It reflects the contribution of baroclinic instability to the formation of eddies in the MIZ. According to the estimate carried out in [31], for Fram Strait and the EGC, instability leading to eddy generation is baroclinic. In addition, in [29], it is concluded that barotropic instability in the central part of Fram Strait is close to zero throughout the year, and baroclinic one is the predominant eddy generation mechanism.

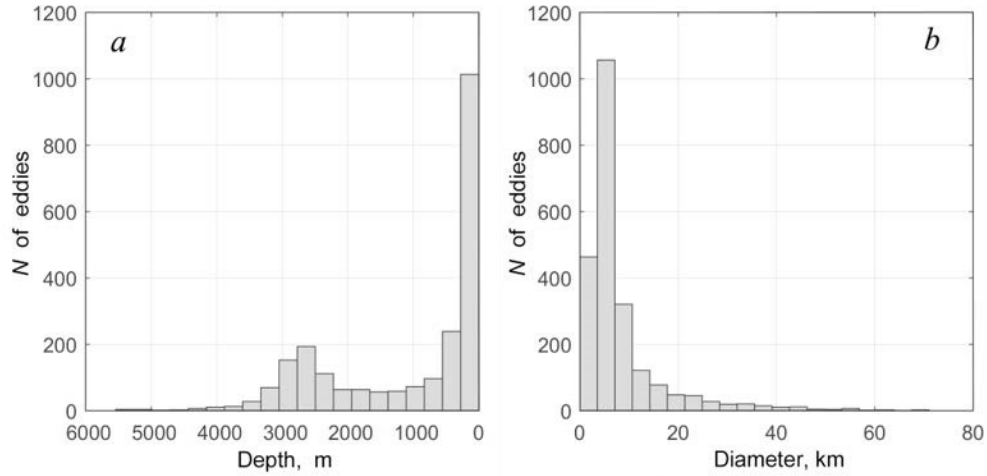

F i g. 9. Distribution histograms of the depths in the eddy manifestation site (*a*) and the eddy diameters (*b*)

As can be seen from Fig. 9, *b*, the largest number of eddies identified in the MIZ (1798) had the dimensions of < 10 km, which is 80% of the total number of structures. Eddies with a diameter of > 30 km (86) account for only 4% of the total number identified. The average value of the parameter is 8.3 km.

The spatial distribution of all identified MIZ eddies is shown in Fig. 10, *a*, in which the size of the marker is proportional to the real diameter of the eddy. It was determined that the diameters varied within the range of 1.3–71.1 km. The number of cyclonic eddies (78%) significantly exceeded the number of anticyclones (22%).

In Fig. 10, *b*, *c*, the spatial distribution of all eddies identified during the study period per given month, and the distribution of their total number per grid cell is demonstrated. As can be seen, the largest number of eddy manifestations occurs at the average seasonal position of the ice distribution boundary in Fram Strait, and southwards from 77°N – on the edge of the eastern Greenland shelf. On the shelf itself, eddies were observed most often over the deepwater area at 77°N.

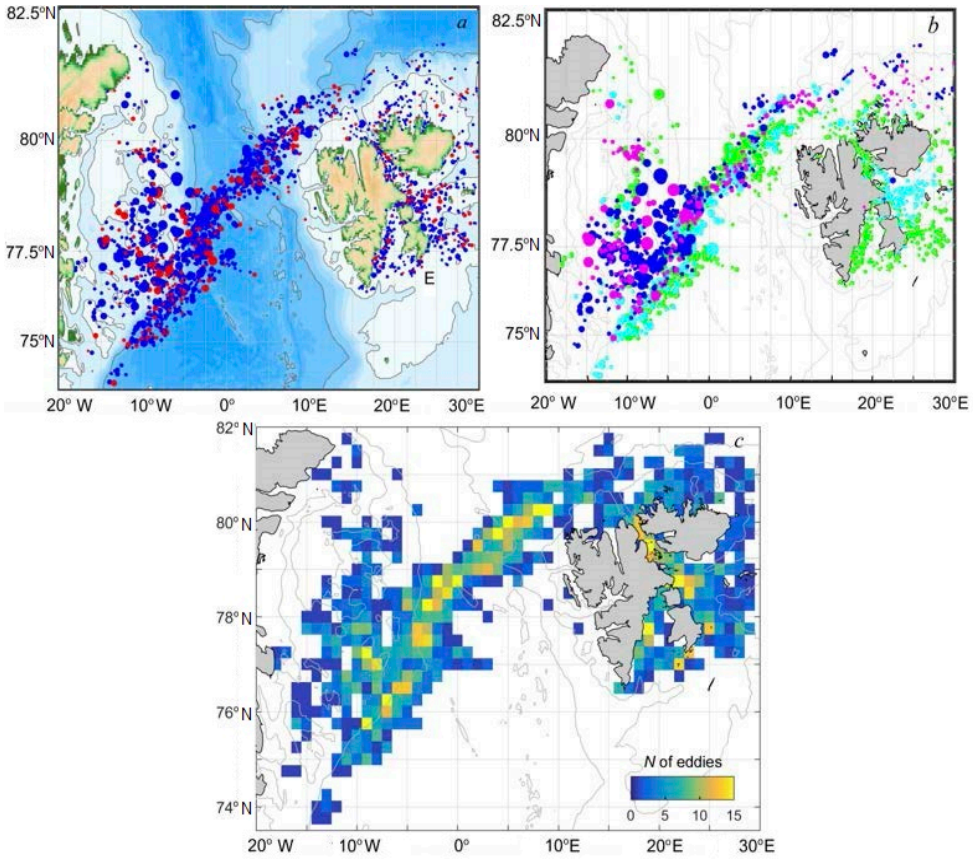

F i g. 10. Spatial distribution of the identified MIZ eddies: *a* – cyclonic (shown in blue) and anticyclonic (shown in red) ones in June – September 2007; *b* – in June (green), July (cyan), August (blue), September (magenta); *c* – total number of the eddy surface manifestations in the marginal ice zone

On the eastern side of Svalbard, the largest number of eddies was recorded in the Hinlopen Strait (due to the long-term preservation of ice in the strait and the presence of islands in it), at the eastern end of the Heleysund Strait (due to its narrowness, leading to damming of waters coming from the ESC), and off the southern coast of Edge Island (as a result of the ESC southern branch interaction with a large number of small islands). Also, increased eddy generation

was noted in the Stur-Fjord Strait along the southeastern shore of Spitsbergen Island in connection with the coastal distribution of the ESC ice and waters. As can be seen in Fig. 10, *b*, these maxima eastwards of Svalbard are associated with eddies recorded exclusively in June – July, and are most likely associated with the presence of melting ice in this area.

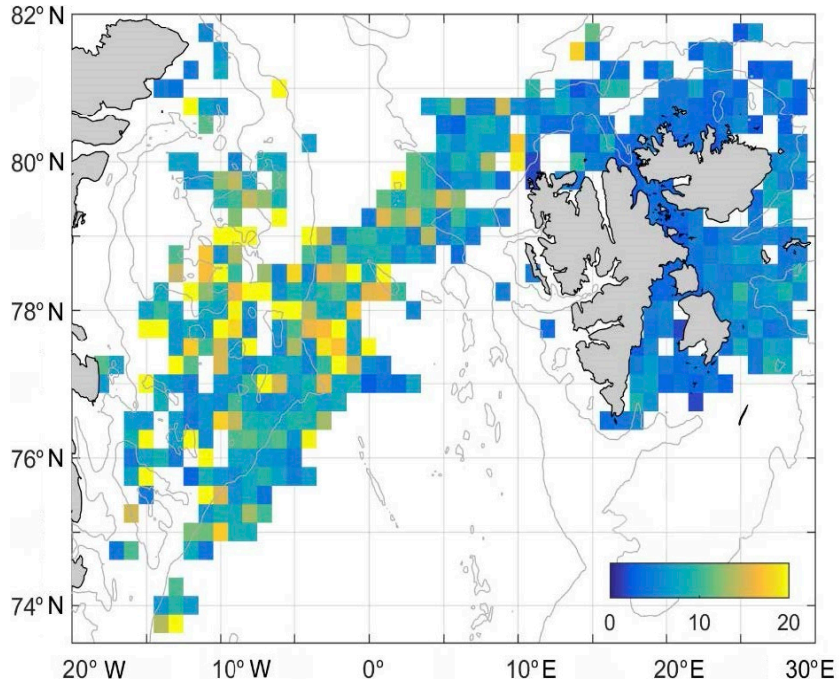

F i g. 11. Mean values of the eddy diameters (km) calculated for each 50 × 50 km grid cell based on satellite SAR measurements for June – September 2007

The spatial distribution of eddy diameters in the MIZ varies depending on the area (Fig. 11). The average diameter of eddies north of Svalbard is ~ 5 km, which is significantly less than in Fram Strait or over the shelf areas of the Greenland Sea with parameter values of 10–20 km. This fact is explained by smaller values of the Rossby deformation radius over the shelf areas of Svalbard [32].

In Fig. 12, the spatial distribution of eddies by month, combined with the positions of the ice boundary at the beginning and end of the month, is given. In general, this figure demonstrates a good spatial correlation between the ice boundary position and the areas of eddy generation.

Eddies of larger diameter are mainly traced on the eastern shelf of the Greenland Sea with a large number of them located along the shelf edge. Most likely, the cause for their origin and development are related to the spread of the AW (recirculation branch of the WSC at 78°N) along the bottom topography features and the advection of warm waters from the south, which, in combination with the wind action, leads to intense mixing and active eddy generation in the form of dipoles. As a result, high frequency of anticyclonic eddy structures is observed in this area, while in other areas the frequency of cyclonic eddies is usually much

higher [8, 30, 33]. In the MD region, the generation of eddies of both rotation signs occurs constantly at the periphery of the quasi-stationary gyre, followed by advection by their currents [2, 21].

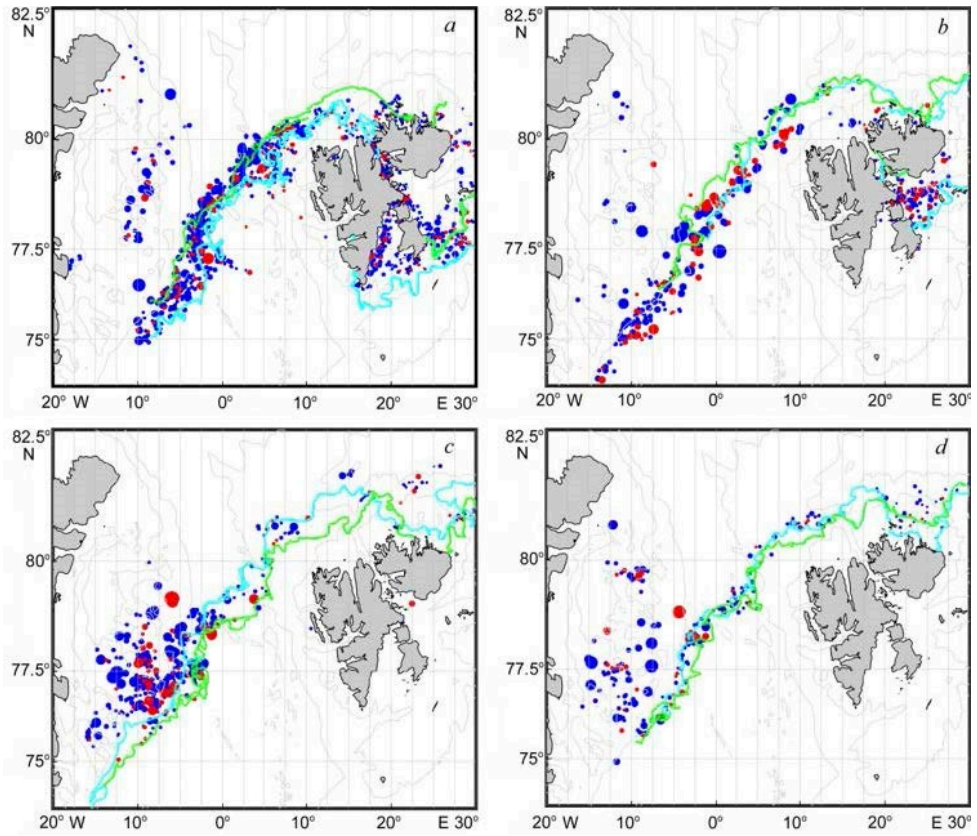

F i g. 12. Distribution of the MIZ eddies and the ice boundary position based on the satellite SAR data for June (*a*), July (*b*), August (*c*), and September (*d*). The blue lines indicate the MIZ position at the beginning of each month and the green ones – at the end of a month

The MIZ eddies observed during the 2007 warm period had a larger diameter in June and July. The ice field edge in Fram Strait underwent significant deformation at that time, which led not only to the active generation of eddies, but also to the formation of well-developed filaments, elongated towards ice-free water and often observed in this area. By the end of the summer season, the diameters of the ice edge eddies decreased, and the ice boundary levelled out and became denser. In September, eddy generation processes at the eastern shelf of Greenland, the peak of which was recorded in August, also weakened.

Conclusions

Analysis of Envisat ASAR satellite radar images in Fram Strait and Svalbard in the 2007 warm period made it possible to identify the features of the ice field edge spatial and temporal variability and the ice field characteristics, as well as the surface manifestations of numerous eddy structures formed in this area.

It was determined that the ice distribution boundary underwent unequal displacements along its entire length. Based on the nature of the variability in the position of the drifting ice field edge, several areas with their own characteristics of eddy generation can be distinguished: the area north of 79°N, the deepwater part of the strait (76–79°N), and the area southwards of 76°N, at which the ice boundary shifts can occur in different directions.

Seasonal ice edge retreat in Fram Strait took place until the beginning of August. North of Svalbard, the ice retreat to the north continued in September. The range of the ice boundary displacements in June – September 2007 varied within 30–220 km, and amounted to more than 4 degrees of latitude (> 450 km) in the southeast.

Under effect of acting winds, the MIZ structure and dimensions change, which also affects the process of eddy generation. At northern winds, the edge is more rarefied and shifted towards open water – the MIZ width increases, and the number of formed eddy structures increases. Westerly winds, i.e., the winds "outward the ice", have a similar effect. At southerly/easterly winds, i.e., the winds "toward the ice", the edge becomes thicker, the width of the MIZ decreases and the number of eddies formed decreases accordingly. A sharp change in wind direction can lead to a fragment of the ice field being detached from the ice edge, trapped into an eddy movement and transported to the open water.

During the study period, an intense eddy generation in the MIZ was revealed. A total of 2272 MIZ eddies were registered, of which 1162 were recorded in June, 420 in July, 451 in August, and 239 in September. The maximum number of identified eddies in June (1162), compared to other months, can be explained by the fact that, by the nature of the processes, June is classified as a more dynamic spring month for the Arctic basin. A slightly larger number of recorded eddies in August (451) compared to July (420) is explained by more active eddy generation at the eastern Greenland Sea shelf, the peak of which was recorded exactly in August.

Larger eddies with the diameter values of 10–20 km were recorded over the Fram Strait deep-sea part and the Greenland Sea eastern shelf, while smaller eddies up to 5 km in diameter were observed mainly over shallow depths near Svalbard. The diameters values varied within the range of 1.3–71.1 km with an average value of 8.3 km. The number of cyclonic eddies (78%) significantly exceeded the number of anticyclones (22%).

It is found that wind conditions have a significant effect on the displacement of the ice edge and the process of eddy generation in the MIZ. Sharp changes of wind direction might lead to the partial breakup of the ice fields. The majority of the identified MIZ eddies has a predominantly cyclonic rotation sign.

REFERENCES

1. Niebauer, H.J. and Smith Jr., W.O., 1989. A Numerical Model of Mesoscale Physical-Biological Interactions in the Fram Strait Marginal Ice Zone. *Journal of Geophysical Research: Oceans*, 94(C11), pp. 16151-16175. doi:10.1029/JC094iC11p16151

2. Kozlov, I.E., Plotnikov, E.V., Manucharyan, G.E., 2020. Brief Communication: Mesoscale and Submesoscale Dynamics in the Marginal Ice Zone from Sequential Synthetic Aperture Radar Observations. *The Cryosphere*, 14(9), pp. 2941-2947. doi:10.5194/tc-14-2941-2020

3. Fine, E.C., MacKinnon, J.A., Alford, M.H. and Mickett, J.B., 2018. Microstructure Observations of Turbulent Heat Fluxes in a Warm-Core Canada Basin Eddy. *Journal of Physical Oceanography*, 48(10), pp. 2397-2418. doi:10.1175/JPO-D-18-0028.1

4. Mensa, J.A., Timmermans, M.-L., Kozlov, I.E., Williams, W.J. and Özgökmen, T.M., 2018. Surface Drifter Observations from the Arctic Ocean's Beaufort Sea: Evidence for Submesoscale Dynamics. *Journal of Geophysical Research: Oceans*, 123(4), pp. 2635-2645. doi:10.1002/2017JC013728

5. Johannessen, O.M., Johannessen, J.A., Morison, J., Farrelly, B.A. and Svendsen, E.A.S., 1983. Oceanographic Conditions in the Marginal Ice Zone North of Svalbard in Early Fall 1979 with an Emphasis on Mesoscale Processes. *Journal of Geophysical Research: Oceans*, 88(C5), pp. 2755-2769. doi:10.1029/JC088iC05p02755

6. Lebedev, K.V., Filyushkin, B.N. and Kozhelupova, N.G., 2019. Argo-Based Study of Water, Heat, and Salt Exchange between Atlantic, Nordic Seas, and Arctic Ocean. *Journal of Oceanological Research*, 47(2), pp. 183-197. doi:10.29006/1564-2291.JOR-2019.47(2).11 (in Russian).

7. Horvat, C., Tziperman, E. and Campin, J.-M., 2016. Interaction of Sea Ice Floe Size, Ocean Eddies, and Sea Ice Melting. *Geophysical Research Letters*, 43(15), pp. 8083-8090. doi:10.1002/2016GL069742

8. Atadzhanova, O.A., Zimin, A.V., Romanenkov, D.A. and Kozlov, I.E., 2017. Satellite Radar Observations of Small Eddies in the White, Barents and Kara Seas. *Physical Oceanography*, (2), pp. 75-83. doi:10.22449/1573-160X-2017-2-75-83

9. Kozlov, I.E., Artamonova, A.V., Manucharyan, G.E. and Kubryakov, A.A., 2019. Eddies in the Western Arctic Ocean from Spaceborne SAR Observations over Open Ocean and Marginal Ice Zones. *Journal of Geophysical Research: Oceans*, 124(9), pp. 6601-6616. doi:10.1029/2019JC015113

10. Kozlov, I.E., Petrenko, L.A. and Plotnikov, E.V., 2019. Statistical and Dynamical Properties of Ocean Eddies in Fram Strait from Spaceborne SAR Observations. In: SPIE, 2019. *Proceedings of SPIE*. Vol. 1150: Remote Sensing of the Ocean, Sea Ice, Coastal Waters, and Large Water Regions 2019, 11150S. doi:10.1117/12.2533317

11. Kozlov, I.E. and Atadzhanova, O.A., 2022. Eddies in the Marginal Ice Zone of Fram Strait and Svalbard from Spaceborne SAR Observations in Winter. *Remote Sensing*, 14(1), 134. doi:10.3390/rs14010134

12. Artamonova, A.V. and Kozlov, I.E., 2023. Eddies in the Norwegian and Greenland Seas from the Spaceborne SAR Observations in Summer, 2007. *Physical Oceanography*, 30(1), pp. 112-123.

13. Khachatrian, E. and Sandalyuk, N., 2022. On the Exploitation of Multimodal Remote Sensing Data Combination for Mesoscale/Submesoscale Eddy Detection in the Marginal Ice Zone. *IEEE Geoscience and Remote Sensing Letters*, 19, 3513805, pp. 1-5. doi:10.1109/LGRS.2022.3215202

14. Khachatrian, E., Sandalyuk, N. and Lozou, P., 2023. Eddy Detection in the Marginal Ice Zone with Sentinel-1 Data Using YOLOv5. *Remote Sensing*, 15(9), 2244. doi:10.3390/rs15092244

15. Kulakov, M.Yu. and Makshtas, A.P., 2013. The Role of Ice Drift in Formation of Sea Ice Cover in the Arctic Ocean at the Beginning of XXI Century. *Arctic and Antarctic Research*, 2, pp. 67-75 (in Russian).

16. Zakharov, V.G. and Kononova, N.K., 2015. Relationship of Dynamics of Fields of Ice Drift in the Arctic Basin and Atmospheric Circulation Northern Hemisphere (Summer Seasons). *The Complex Systems*, 1(2), pp. 45-57.

17. Ogi, M. and Wallace, J.M., 2012. The Role of Summer Surface Wind Anomalies in the Summer Arctic Sea Ice Extent in 2010 and 2011. *Geophysical Research Letters*, 39(9), L09704. doi:10.1029/2012GL051330

18. Ogi, M., Rigor, I.G., McPhee, M.G. and Wallace, J.M., 2008. Summer Retreat of Arctic Sea Ice: Role of Summer Winds. *Geophysical Research Letters*, 35(24), L24701. doi:10.1029/2008GL035672

19. Stroeve, J.C., Serreze, M.C., Holland, M.M., Kay, J.E., Malanik, J. and Barrett, A.P., 2012. The Arctic's Rapidly Shrinking Sea Ice Cover: a Research Synthesis. *Climatic Change*, 110, pp. 1005-1027. doi:10.1007/s10584-011-0101-1

20. Kwok, R. and Cunningham, G.F., 2008. ICESat over Arctic Sea Ice: Estimation of Snow Depth and Ice Thickness. *Journal of Geophysical Research: Oceans*, 113(C8), C08010. doi:10.1029/2008JC004753

21. Johannessen, J.A., Johannessen, O.M., Svendsen, E., Shuchman, R., Manley, T., Campbell, W.J., Josberger, E.G., Sandven, S., Gascard, J.C. [et al.], 1987. Mesoscale Eddies in the Fram Strait Marginal Ice Zone during the 1983 and 1984 Marginal Ice Zone Experiments. *Journal of Geophysical Research: Oceans*, 92(C7), pp. 6754-6772. doi:10.1029/JC092iC07p06754

22. Hopkins, T.S., 1991. The GIN Sea–A Synthesis of Its Physical Oceanography and Literature Review 1972–1985. *Earth-Science Reviews*, 30(3-4), pp. 175-318. doi:10.1016/0012-8252(91)90001-V

23. Pérez-Hernández, M.D., Pickart, R.S., Pavlov, V., Våge, K., Ingvaldsen, R., Sundfjord, A., Renner, A.H.H., Torres, D.J. and Erofeeva, S.Y., 2017. The Atlantic Water Boundary Current North of Svalbard in Late Summer. *Journal of Geophysical Research: Oceans*, 122(3), pp. 2269-2290. doi:10.1002/2016JC012486

24. Bourke, R.H., Tunnicliffe, M.D., Newton, J.L., Paquette, R.G. and Manley, T.O., 1987. Eddy near the Molloy Deep Revisited. *Journal of Geophysical Research: Oceans*, 92(C7), pp. 6773-6776. doi:10.1029/JC092iC07p06773

25. Hattermann, T., Isachsen, P.E., von Appen, W.-J., Albretsen, J. and Sundfjord, A., 2016. Eddy-Driven Recirculation of Atlantic Water in Fram Strait. *Geophysical Research Letters*, 43(7), pp. 3406-3414. doi:10.1002/2016GL068323

26. Liu, A.K., Häkkinen, S. and Peng, C.Y., 1993. Wave Effects on Ocean-Ice Interaction in the Marginal Ice Zone. *Journal of Geophysical Research: Oceans*, 98(C6), pp. 10025-10036. doi:10.1029/93JC00653

27. Watkins, D.M., Bliss, A.C., Hutchings, J.K. and Wilhelmus, M.M., 2023. Evidence of Abrupt Transitions between Sea Ice Dynamical Regimes in the East Greenland Marginal Ice Zone. *Geophysical Research Letters*, 50(15), e2023GL103558. doi:10.1029/2023GL103558

28. Atadzhanova, O.A., Zimin, A.V., Svergun, E.I. and Konik, A.A., 2018. Submesoscale Eddy Structures and Frontal Dynamics in the Barents Sea. *Physical Oceanography*, 25(3), pp. 220-228. doi:10.22449/1573-160X-2018-3-220-228

29. Wekerle, C., Wang, Q., von Appen, W.-J., Danilov, S., Schourup-Kristensen, V. and Jung, T., 2017. Eddy-Resolving Simulation of the Atlantic Water Circulation in the Fram Strait with Focus on the Seasonal Cycle. *Journal of Geophysical Research: Oceans*, 122(11), pp. 8385-8405. doi:10.1002/2017JC012974

30. Bashmachnikov, I.L., Kozlov, I.E., Petrenko, L.A., Glok, N.I. and Wekerle, C., 2020. Eddies in the North Greenland Sea and Fram Strait from Satellite Altimetry, SAR and High-Resolution Model Data. *Journal of Geophysical Research: Oceans*, 125(7), e2019JC015832. doi:10.1029/2019JC015832

31. Wadhams, P. and Squire, V.A., 1983. An Ice-Water Vortex at the Edge of the East Greenland Current. *Journal of Geophysical Research: Oceans*, 88(C5), pp. 2770-2780. doi:10.1029/JC088iC05p02770

32. Nurser, A.J.G. and Bacon, S., 2014. The Rossby Radius in the Arctic Ocean. *Ocean Science*, 10(6), pp. 967-975. doi:10.5194/os-10-967-2014

33. Petrenko, L.A. and Kozlov, I.E., 2020. Properties of Eddies near Svalbard and in Fram Strait from Spaceborne SAR Observations in Summer. *Sovremennye Problemy Distantsionnogo Zondirovaniya Zemli iz Kosmosa*, 17(7), pp. 167-177. doi:10.21046/2070-7401-2020-17-7-167-177 (in Russian).

About the authors:

Larisa A. Petrenko, Junior Research Associate, Marine Hydrophysical Institute of RAS (2 Kapitanskaya Str., Sevastopol, 299011, Russian Federation), **WoS ResearcherID: AAY-6398-2020**, **Scopus Author ID: 7004614243**, **ORCID ID: 0000-0001-7246-9885**, **SPIN-code: 1478-6492 AuthorID: 854482**, larcpetr@gmail.com

Igor E. Kozlov, Leading Research Associate, Marine Hydrophysical Institute of RAS (2 Kapitanskaya Str., Sevastopol, 299011, Russian Federation), Ph.D. (Phys.-Math.), **ORCID ID: 0000-0001-6378-8956**, **ResearcherID: G-1103-2014**, **Scopus Author ID: 49963767500**, ik@mhi-ras.ru

Contribution of the co-authors:

Larisa A. Petrenko – problem formulation and statement, analysis of materials on the research topic, processing and describing the research results, preparing the text of the paper and graphic material

Igor E. Kozlov – general scientific supervision of the research, preparation of graphic material, editing and supplementing the text of the paper

The authors have read and approved the final manuscript.
The authors declare that they have no conflict of interest.